

## WHAT DO WE LEARN FROM (e,e'p) EXPERIMENTS

S. Gilad<sup>1,†</sup>

<sup>1</sup>*Massachusetts Institute of Technology, Cambridge, MA, USA*

The promise and limitations of studying nuclear structure and reactions using (e,e'p) reactions are discussed. A(e,e'p)A-1 reactions on complex nuclei are used to test new relativistic mean-field calculations and their ingredients such as ground-state wave function, current operators, final-state interactions and two-body currents, and to assess the limits of single-particle models. For higher excitations of the residual nuclei, A(e,e'p) reactions reveal only qualitative features of the reaction mechanism, and their increased usefulness awaits input from more complex reactions such as A(e,e'X). The (e,e'p) experiments on few-body nuclei provide essential input to quickly developing theories for few-body systems, where individual theoretical ingredients can be studied very selectively. A large data set is needed for this purpose, and existing or proposed experimental programs are discussed. If hadronic theories can meet the challenge of consistently describing this body of data at low and moderate energies, the transition from hadronic to quark-gluon degrees of freedom could be probed in experiments at higher energies.

### 1. INTRODUCTION

Exclusive A(e,e'p)A-1 reactions have been used in the last two decades to study nuclear structure. Cross-sections have been measured for specific states of the residual nuclei as a function of the missing momentum,  $p_m$ . The electron-nucleon cross-section was then divided out of the measured cross-sections to extract the “distorted” momentum distribution for a specific hole state. The data, mainly for low transferred momenta ( $Q^2 \leq 0.4$  (GeV/c)<sup>2</sup>), have been analyzed in terms of non-relativistic model-dependent DWIA calculations. The final-state interactions (FSI) of the ejected nucleons were treated by optical potentials with parameters generally obtained by fitting p-(A-1) elastic scattering data. Some of these calculations include also contributions to the cross-sections from two-body currents such as meson-exchange currents (MEC) and isobar configurations (IC). DWIA calculations generally describe well the shape of the measured distorted momentum distributions of valence states for missing momenta up to 250 – 300 MeV/c, but the calculated magnitudes are higher than those measured. For any specific hole state, the ratio between the measured and the calculated cross-section gives the occupancy (or spectroscopic factor) of the state in comparison to mean-field single-particle models predictions. For nuclei with  $A > 4$ , for which mean-field calculations have been used, the measured occupancy (see Fig. 1) is approximately 0.6 [1].

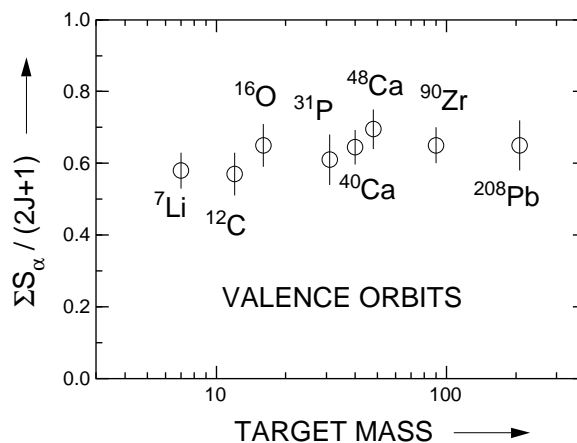


FIG. 1: Spectroscopic factors for valence states of different nuclei. These spectroscopic factors were extracted using the independent particle shell model (IPSM) [1].

<sup>†</sup>Electronic address: sgilad@mitlns.mit.edu

The low occupancy has been attributed to shifted strength from single-particle states to more complicated configurations and nucleon-nucleon correlations. For missing momenta higher than 300 MeV/c, as well as for high missing (excitation) energies, DWIA under-predicts the measured cross-sections, supporting this hypothesis.

In the last several years, new experimental facilities and theoretical advances have come into being. High-quality continuous-wave (CW) beams as well as high-resolution spectrometers provide very detailed and precise new data up to transferred momenta above 1 (GeV/c)<sup>2</sup>. Theoretically, fully relativistic DWIA calculations are now available for mean-field approaches to many-body nuclei [2], while microscopic calculations with increasingly more relativistic ingredients are used for few-body systems [3, 4, 5]. It is possible now, therefore, to study nuclei and nuclear reactions in great detail. Thus, response functions and a variety of kinematics provide selectivity in the contributions due to various currents. We are in a position, then, to constrain our models and explicitly test their ingredients.

This manuscript is written in light of these developments. We do not attempt to provide a review of all (e,e'p) experiments. Rather, we examine the promise and limitations in using them to study both nuclear structure and nuclear reactions. We limit ourselves here to study of nuclei (i.e.  $A \geq 2$ ). Furthermore, although polarization observables are now routinely used in (e,e'p) reactions, we deal here with reactions for which the only polarization observable is the beam-helicity asymmetry.

## 2. (e,e'p) ON COMPLEX NUCLEI

A beautiful example of the success and limitations of previous studies of complex nuclei is illustrated in Fig. 2 from reference [6]. The missing-momentum distributions of low-lying states in the reaction  $^{208}\text{Pb}(e,e'p)^{207}\text{Tl}$  that have been measured in two experiments at NIKHEF are compared to several non-relativistic DWIA calculations. The low  $p_m$  data were measured in parallel kinematics, whereas the data for  $300 \text{ MeV}/c \leq p_m \leq 500 \text{ MeV}/c$  were measured at constant electron kinematics. Since the purpose of the measurement was to look for correlations in the ground-state wave function, most calculations [8, 9, 10] used a variety of prescriptions to account for long-range and short-range correlations (SRC).

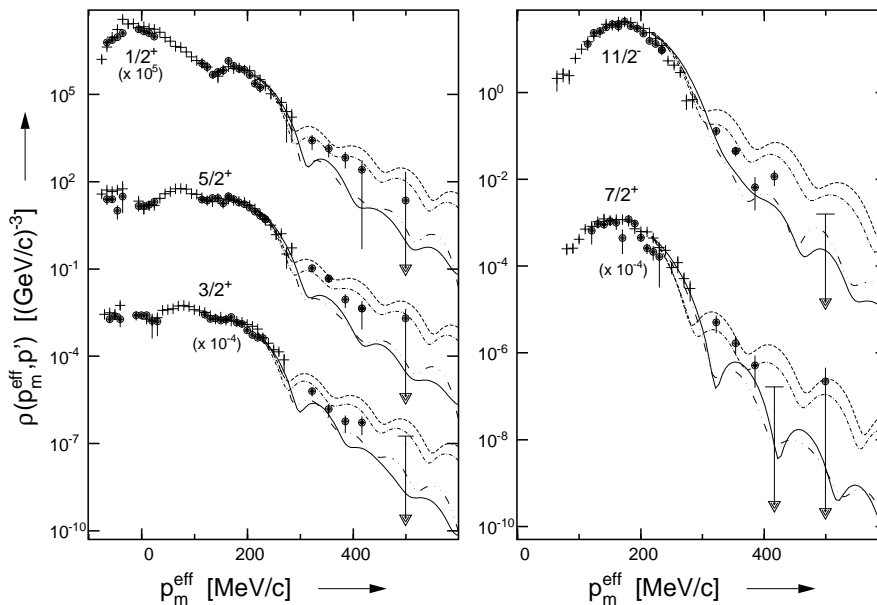


FIG. 2: Missing momentum distributions for low-lying states in the reaction  $^{208}\text{Pb}(e,e'p)^{207}\text{Tl}$ . Solid circular data are from Bobeldijk *et al.* [6], and the plus data are from Quint *et al.* [7]. The solid lines are DWIA calculations. Calculations that include correlations are by Pandharipande [8] (dash-double-dotted), Ma and Wambach [9] (dashed) and Mahaux and Sartor [10] (dot-dashed).

As can be seen, all DWIA calculations reproduce the data well up to  $p_m = 300$  MeV/c. However, only qualitative conclusions could be drawn as to the apparent effect of long-range correlations at low excitation energies, demonstrating the need for additional observables to constrain the models. A case in point is a subsequent analysis of the same data [11] in which fully relativistic mean-field DWIA calculations without correlations have been used to consistently account for the observed missing-momentum distributions below and above 300 MeV/c. In what has been a general trend, the spectroscopic factors extracted from the relativistic analysis are higher than those extracted from the non-relativistic calculations. Following the suggestion of Mütter and Dickhoff [12] that short-range and tensor correlations should be present at high missing momenta and high excitation energies, further measurements were performed in this kinematic region [13].

In a more recent experiment, J. Gao et al. measured the reaction  $^{16}\text{O}(e,e'p)^{15}\text{N}$  [14]. Cross-sections to the two valence  $1p$ -shell states, as well as response functions were measured in quasielastic kinematics and  $Q^2 = 0.8$  (GeV/c)<sup>2</sup> at the Jefferson Laboratory (JLab). In Fig. 3a the measured cross-sections to the two  $1p$ -shell states up to  $p_m = 350$  MeV/c are presented together with fully relativistic DWIA calculations by Udias et al. [15] and “relativized” DWIA calculations by Kelly [16]. The data were measured at a constant electron kinematics and are very precise up to the highest missing momentum. Both calculations use NLSH bound-state wave functions. However, while Udias solves the Dirac equation directly, the calculations by Kelly use the effective momentum approximation for the lower components of the Dirac spinors. It is evident that the fully relativistic calculations better describe the data at the highest missing momenta. The spectroscopic factors are 0.73 and 0.72 for the  $1p_{1/2}$  and 0.71 and 0.67 for the  $1p_{3/2}$  state for the Udias and Kelly calculations, respectively. The somewhat higher spectroscopic factors than the ones in Fig. 1 are a common feature of relativistic calculations, and suggest that a larger component of the wave function can be understood in terms of relativistic mean-field models.

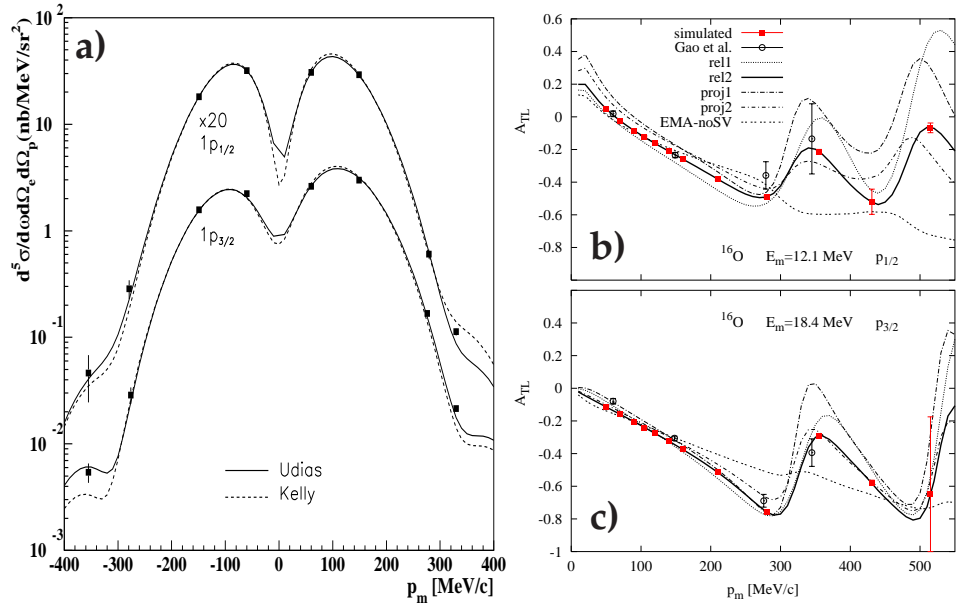


FIG. 3: a) Measured cross-sections by Gao et al. [14] and DWIA calculations by Udias et al. [15] and Kelly [16] of the  $^{16}\text{O}(e,e'p)^{15}\text{N}$  reaction. b) Measured and calculated  $A_{LT}$  asymmetry for the  $1p_{1/2}$  state. See text for details. c) Same as b) but for the  $1p_{3/2}$  state.

The importance of dynamical relativistic effects is further illustrated in Fig. 3b and Fig. 3c. Fig. 3b shows the measured and calculated  $A_{LT}$  asymmetry for the  $1p_{1/2}$  and Fig. 3c shows the same for the  $1p_{3/2}$  state. All calculations are by Udias. The rel1 and rel2 are the fully relativistic calculations that use de Forest [17] cc1 and cc2 current operators respectively, the “proj” indicate that momentum-dependent positive energy projection operator was employed, while the EMA-noSV indicates that the effective momentum approximations was used and no spinor distortions were permitted. The rel2 calculations are the same as in Fig. 3a. It is clear from the figures that

spinor distortions arising from the enhancement of the lower components due to the scalar and vector potentials are necessary to adequately describe the structure of the observed  $A_{LT}$  asymmetries. The  $R_{LT}$ ,  $R_L$  and  $R_T$  which were measured by Gao *et al.* are reproduced as well [14] by Udias’ calculations, whose only adjustable parameter was the spectroscopic factor. It strongly suggests that in these calculations, we have a successful model for single-particle description of  $A(e,e'p)A-1$  reactions on complex nuclei. That said, there is a need to test the limits of this model for high missing momenta, and the “simulated data points” (full squares) in Figs. 3b,c are predicted values of the  $A_{LT}$  asymmetries up to missing momenta of 550 MeV/c using the same model by Udias. These, as well as the cross-sections to  $p_m = 700$  MeV/c will be measured at JLab in 2001 [18]. It is noteworthy that work is in progress to include MEC into these  $A(e,e'p)A-1$  relativistic calculations [19, 20]. Other work is being done to consolidate the use of optical potentials with that of the eikonal approximation for the treatment of FSI [21].

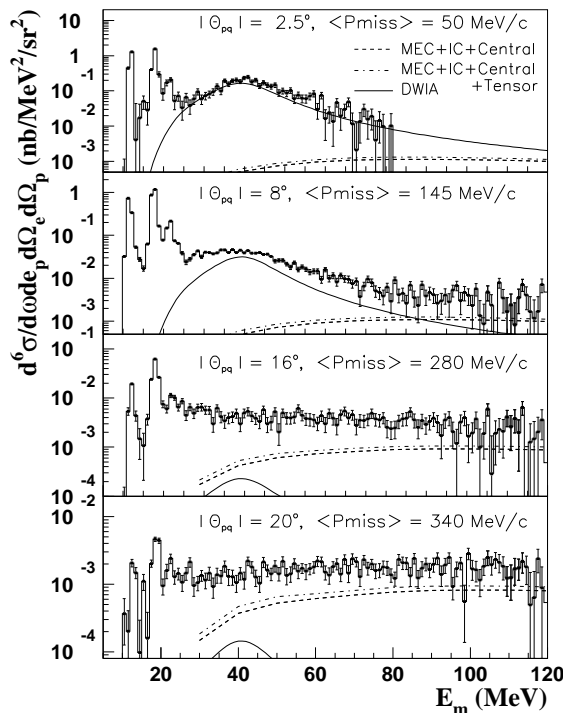


FIG. 4: Cross-sections as functions of missing energies for different missing momenta. DWIA are calculations by Kelly [16] in which the  $1s$ -shell strength is folded with the Lorentzian parameterization by Mahaux. The dashed and dot-dashed curves are calculations by Ryckebusch *et al.* [23] of the contributions to the  $^{16}\text{O}(e,e'p)$  cross-section from  $^{16}\text{O}(e,e'np)$  and  $^{16}\text{O}(e,e'pp)$ . (See text for details.)

It is already evident that  $A(e,e'p)$  reactions on complex nuclei to high missing (excitation) energies provide only qualitative information, and mainly on the reaction mechanism. A recent measurement of the  $^{16}\text{O}(e,e'p)$  reaction [22] at JLab at  $Q^2 = 0.8$   $(\text{GeV}/c)^2$  clearly illustrates this point. The cross-sections for missing energies ranging from the  $1s_{1/2}$  hole state to 120 MeV were measured at missing momenta of 50-340 MeV/c. The data are presented in Fig. 4 and compared to the same single-particle “relativized” DWIA calculations by Kelly [16] that are reasonably successful for the  $1p$  states (see Fig. 3a). The spectroscopic factor was 0.73. It is strikingly clear that a proton knockout from the  $1s_{1/2}$  shell accounts for the cross-section at  $p_m = 50$  MeV/c, but the contribution to the cross-sections from  $1s_{1/2}$  knockout decreases fast with increasing missing momentum, and at  $p_m = 200$  MeV/c, it is less than 10 percent. Above this  $p_m$ , the cross-sections are approximately flat for  $E_m > 25$  MeV.

Also presented in the figure are calculations in a Hartree-Fock framework by Ryckebusch *et al.* [23] of the contributions to the  $^{16}\text{O}(e,e'p)$  cross-section from  $^{16}\text{O}(e,e'np)$  and  $^{16}\text{O}(e,e'pp)$  due

to MEC, IC and central (Jastrow) and tensor correlations. All these contributions can only account for about a half of the observed cross-sections at high missing momenta. In these calculations, two-body (MEC and IC) currents constitute about 85% of the calculated  $^{16}\text{O}(e,e'pp)$  and  $^{16}\text{O}(e,e'np)$  contributions, tensor short-range correlations are about 13% and central SRC are only 2%. The large contribution from two-body currents is consistent with the measured response functions that were separated by Liyanage *et al.* [22] as well. The cross-sections at high missing energies are more transverse than predicted by DWIA for single-particle states, and increasingly so with increasing missing momentum. Excess transverse cross-sections at high  $E_m$  had been previously measured for  $^{12}\text{C}$  by Ulmer *et al.* [24] at  $Q^2 = 0.15$  (GeV/c)<sup>2</sup> and Dutta *et al.* [25] at  $Q^2 = 0.64$  and 1.8 (GeV/c)<sup>2</sup>. Dutta’s observation that the excess transversity decreases with  $Q^2$  is consistent with Liyanage’s results as well.

Although a qualitative picture emerges from studying the dynamics of  $A(e,e'p)$  reaction at high missing energies, models are far from being consistent and quantitative because the task of disentangling reactions effects (FSI, MEC, IC etc.) from contributions to the wave function from N-N correlations is too complex for the  $(e,e'p)$  reaction alone. Hopefully, data from other reaction channels such as  $A(e,e'pp)$ ,  $A(e,e'np)$  and  $A(e,e'X)$ , where X is any combination of hadrons, can provide qualitative and quantitative knowledge on the channels contributing to the  $A(e,e'p)$  reaction. With such input, it may be possible to shed light on the elusive subject of short-range correlations. Such experiments are being now performed, but they are outside of the scope of this manuscript.

### 3. (e,e'p) ON FEW-BODY SYSTEMS

From a strictly experimental point of view, the use of  $A(e,e'p)$  reactions to study few-body nuclear systems is not different from the study of complex nuclei. However, there are differences in the theoretical treatments that affect the present and future possibilities and limitations associated with these reactions.

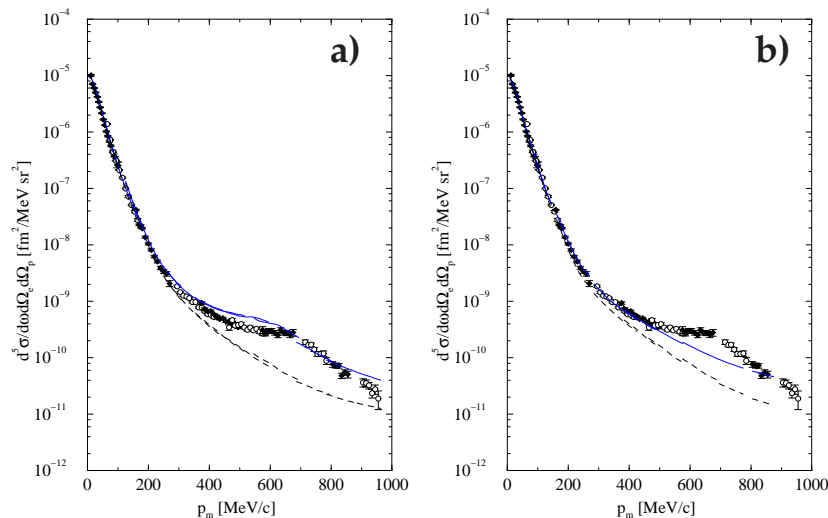


FIG. 5: Measured and calculated  $d(e,e'p)$  cross-sections. In both panels, the solid curves are calculations that include MEC and IC, and the dashed curves are calculations that do not include contributions from two-body currents. a) Calculations by Arenhövel (private communications in [26]). b) Calculations using a code by Schiavilla (private communications in [26]).

The electrodisintegration of the deuteron,  $^2\text{H}(e,e'p)n$ , has been used to study N-N potentials, the structure of the deuteron and reaction dynamics. Fig. 5 presents results from a recent experiment at MAMI [26]. Cross-section over a range of 6 orders of magnitude were measured with high precision as a function of missing (recoil) momentum up to  $p_m = 950$  MeV/c. Because of the low beam energy of the MAMI microtron, this measurement could not be performed at a constant electron kinematics, hence imposing ambiguities on the theoretical interpretation of the data.

Nevertheless, such a measurement that was impossible only ten years ago, provides invaluable and badly needed input to reaction models. The higher beam energy available at JLab makes it possible to perform a similar measurement at a constant electron kinematics, eliminating some ambiguities from the theoretical interpretation.

Also presented in the two panels of Fig. 5 are two state-of-the-art calculations by Arenhövel and Schiavilla, each with and without MEC and IC. In both calculations the clear importance of including these two-body currents for reproducing even the gross features of the cross-sections above  $p_m = 300$  MeV/c is evident. Since these high  $p_m$  data were measured at  $\Delta$  kinematics, the contributions from IC are more important than those from MEC. Yet, the two calculations are very different in treating the two-body currents and produce different calculated cross sections. This is a clear indication that a measurement of a single observable (cross-sections in this case) is insufficient to fully disentangle the contributing ingredients. As many observables as possible, and at more than one kinematics are necessary for this purpose.

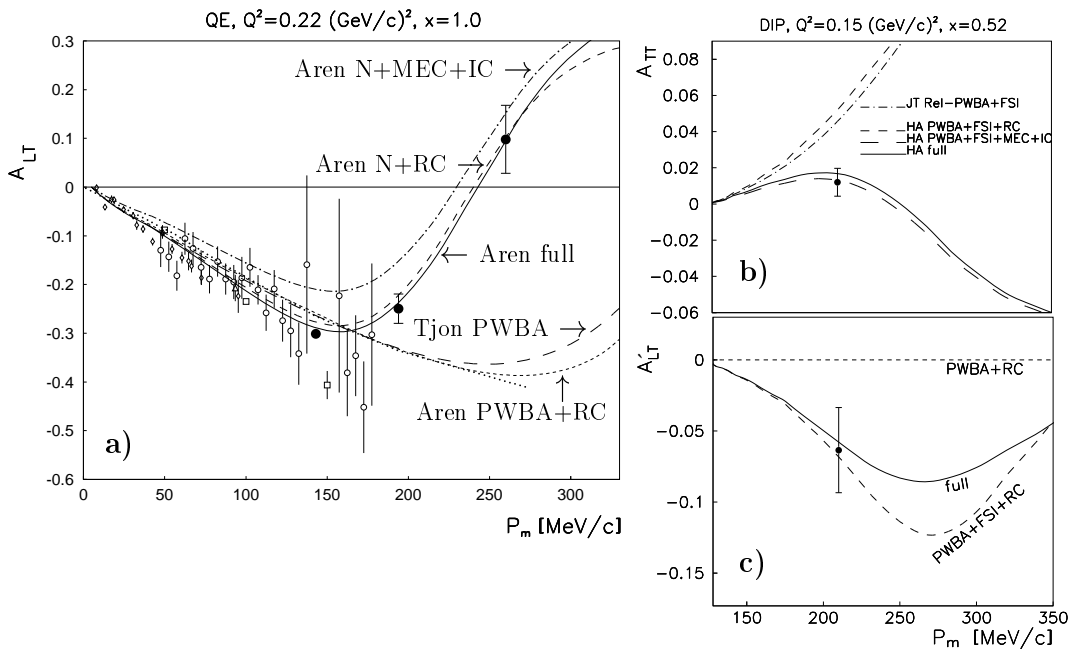


FIG. 6: Interference asymmetries for the  ${}^2\text{H}(e,e'p)n$  reaction. The solid circles are data from reference [28]. The open circles are previous data. The calculations by Tjon are fully relativistic. The calculations by Arenhövel are based on the Schrödinger equation and include relativistic corrections. The dotted curve is the  $cc1$  current operator as prescribed by de Forest [17]. a)  $A_{LT}$  in quasielastic kinematics. b)  $A_{TT}$  in dip kinematics. c)  $A'_{LT}$  in dip kinematics.

An example of an attempt to disentangle the model ingredients in the  ${}^2\text{H}(e,e'p)n$  reaction is the program at the MIT-Bates Linear Accelerator Center to measure the four helicity-independent unpolarized response functions  $R_L$ ,  $R_T$ ,  $R_{LT}$ ,  $R_{TT}$  and the (“fifth”) helicity-dependent response  $R'_{LT}$ . Since the two latter responses require the detections of the knocked-out proton out of the electron-scattering plane, a system was constructed of four out-of-plane magnetic spectrometers (OOPS) [27] that can be positioned around the momentum-transfer vector, each with a precision better than  $\pm 0.3$  mm and  $\pm 0.3$  mrad. Initial results at  $Q^2 = 0.22$  (GeV/c) $^2$  [28] of the interference  $A_{LT}$  asymmetry at quasielastic kinematics and at  $Q^2 = 0.15$  of the interference  $A_{TT}$  and  $A'_{LT}$  asymmetries in dip kinematics are presented in Fig. 6 together with calculations by H. Arenhövel and J. Tjon. The sensitivity of each response to the various ingredients is clearly demonstrated in the figure.  $A_{LT}$  is very sensitive to relativistic effects (as already noted above for  ${}^{16}\text{O}(e,e'p){}^{15}\text{N}$ ). Yet, since Tjon’s relativistic calculations do not include contributions from FSI, they fail to reproduce the data.  $A_{TT}$  is sensitive mainly to two-body currents, whereas  $A'_{LT}$  is mainly sensitive to FSI. Furthermore, dip kinematics enhances the contributions from two-body currents, while  $\Delta$

kinematics is expected to emphasize IC over MEC. Hence, precise and simultaneous measurements of all these responses at the various kinematics constrain the models to the point that all ingredients have to be treated correctly. In the initial results of Fig. 6, the calculations by Arenhövel are able to reproduce all the data. It remains to be seen whether these calculations are able to reproduce future data at a higher  $p_m$  and at  $\Delta$  kinematics, from measurements that are planned at Bates [29].

The  $R_L$  and  $R_T$  responses have been measured using the “Rosenbluth separation” method, whereby the cross-sections are measured in parallel kinematics for constant transferred momentum and energy at two electron angles (virtual photon polarizations). At  $p_m = 50$  MeV/c, results from Saclay and Bates are not consistent with those from NIKHEF [30] in that their measured  $R_L$  is lower by about 40%. Moreover, their measured  $R_L$  response is about 20% lower than predicted by Arenhövel’s calculations. Preliminary data from a more recent measurement at Mainz [31] also indicates a smaller  $R_L$  than predicted. This poses a huge problem, since there is very little room in the theory to adjust the  $R_L$  response. It has been suggested that the discrepancy between the measured and predicted  $R_L$  may be due to the fact that measurements in parallel kinematics are prone to large uncertainties due to the correlation between  $p_m$  and the transferred energy, and at low  $p_m$  also due to ambiguities in the definition of the  $\vec{p}_m$  vector. Consequently, an alternative “Rosenbluth separation” was proposed at Bates using perpendicular kinematics. Although in perpendicular-kinematics “Rosenbluth separation”  $R_L$  is contaminated by a small contribution from  $R_{TT}$ , this  $R_{TT}$  contribution can be directly and simultaneously measured using OOPS, providing a clean and alternative measure of the  $R_L$  response.

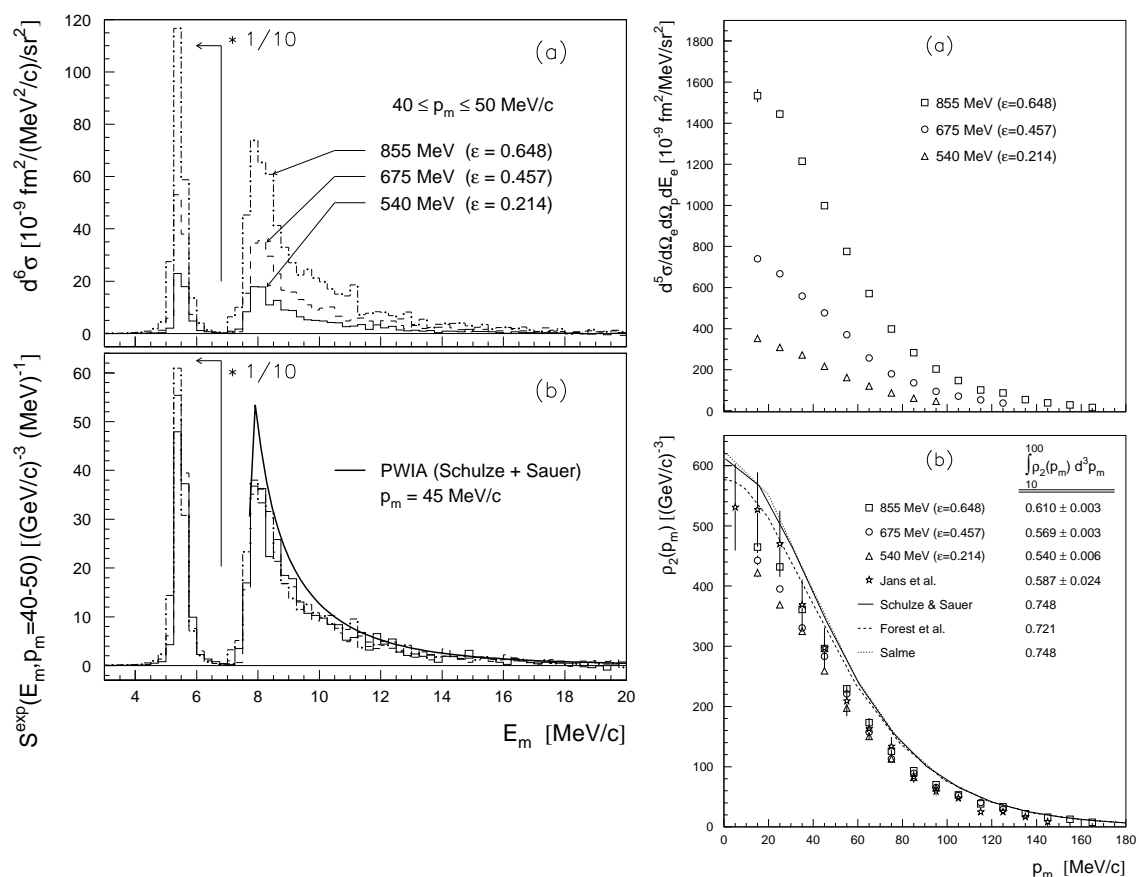


FIG. 7: Left panel: a)  $^3\text{He}(e,e'p)$  cross-sections and b) experimental (“distorted”) spectral functions of missing energy for a missing momentum bin of 40-50 MeV/c. Right panel: a)  $^3\text{He}(e,e'p)^2\text{H}$  cross-sections as a function of missing momentum. b) extracted (“distorted”) momentum distributions for the two-body breakup process compared to various calculations. Figures b (left and right) were obtained by dividing out the electron-proton cross sections from the data in figures a (left and right), respectively. The figures are from reference [32].

Data are also available on  ${}^3\text{He}(e,e'p)$  and  ${}^4\text{He}(e,e'p)$ . The cross-sections and the  $R_L$ ,  $R_T$  and  $R_{LT}$  responses were measured for both nuclei. However, by and large, they were measured in sporadic kinematics, making a consistent theoretical interpretation difficult. Nevertheless, it is worth mentioning the example of a program at MAMI [33] to measure the  $R_L$  and  $R_T$  responses for  ${}^3\text{He}(e,e'p)$  and  ${}^4\text{He}(e,e'p)$  in the same transferred momentum and for three transferred energies on, above and below the quasielastic peak. The idea is to selectively emphasize the single particle aspects of the reaction in quasielastic kinematics, MEC and IC in dip kinematics and SRC below the quasielastic peak ( $x_B > 1$ ). The data for  ${}^3\text{He}(e,e'p)$  in quasielastic kinematics have been published [32] with the main conclusions that the L/T behavior of the cross-section follows that of the electron-proton's, and that MEC and IC do not play a noticeable role in this cross-section. Fig. 7 demonstrates the first conclusion.

Results for the quasielastic  ${}^4\text{He}(e,e'p)$  measurement are soon to be submitted for publication and show similar L/T behavior, as do results for  ${}^3\text{He}(e,e'p)$  at  $x_B > 1$  [34]. For both nuclei, the  $R_{LT}$  response was also measured at MAMI for a variety of transferred momenta and the results will be published upon completion of the analysis.

With the availability of high-energy, high quality beams and detectors with large acceptance and high precision it is possible now to look for the transition from hadronic to quark-gluon (or quark and flux tubes) degrees of freedom in the nucleus. The idea is to reach the limit of being able to describe a large data set with “conventional” nuclear physics. For this purpose it is necessary, and work is underway, to develop what theorists refer to as a “standard model of nuclear physics”, that includes a consistent treatment of FSI, two-body currents, and relativity (wave-functions, current operators and dynamics). Because of the deuteron's simplicity, the  ${}^2\text{H}(e,e'p)n$  reaction at high energies and transferred momenta can be used as a unique laboratory for this study. A program is pending at JLab [35] to test the models that are being developed by measuring the cross-sections and responses of the  ${}^2\text{H}(e,e'p)n$  reaction at high energies and transferred momenta and at a variety of kinematics. However, such studies cannot be confined to the deuteron, if a consistent theory is to be developed. A similar program for  ${}^3\text{He}(e,e'p)$  is already underway [36], with preliminary data to be presented in the Fall 2001 DNP meeting in Hawaii. A proposal for  ${}^4\text{He}(e,e'p)$  has been approved by the JLab PAC as well [37]. Data on  ${}^4\text{He}$  will have an added importance, as they can provide a bridge between microscopic and mean-field  $A(e,e'p)$  calculations. With the above in mind, the immediate limitations of  $(e,e'p)$  experiments at high energies and transferred momenta will be due to theoretical interpretation. In turn, theoretical progress can only be made if high quality data on a rich set of observables are available to constrain and test it.

#### 4. SUMMARY

$(e,e'p)$  is a powerful tool for studying nuclear structure and interactions. High quality and consistent data on many observables and at a variety of kinematics are needed to constrain and test theoretical models. Fortunately, we are at a stage where such data are feasible to obtain, and indeed are beginning to emerge. Simultaneously, theoretical models are being developed in which relativity, modern approaches in treating correlations, FSI and two-body currents as well as sophisticated computational techniques play increasingly important roles.

For many-body nuclei relativistic mean-field DWIA calculations are very successful in predicting cross-sections and responses in  $A(e,e'p)A-1$  up to missing momenta of 350 MeV/c. Measurements are pending to determine the  $p_m$  limits of this model, while work is also being done to include two-body currents in this model. For higher residual excitations, the usefulness of  $A(e,e'p)$  reactions is limited by the complexity of channels contributing to the reaction. Such reaction channels must be measured explicitly in order to provide additional input for the analysis of the  $A(e,e'p)$  channel. It is anticipated that the next-generation MAMI accelerator, with its high-quality 1.5 GeV beam will play a central role in the study of complex nuclei.

Theories are developing faster in the few-body sector. Exact non-relativistic calculations are available for the deuteron and  ${}^3\text{He}$ , and variational Monte Carlo techniques are used for  ${}^{3,4}\text{He}$ . Two-body currents are treated in all calculations, including the Faddeev-based calculations for the three-nucleon system. Relativity is included to various degrees in all calculations, either as corrections or explicitly. Relativistic current operators and, in some cases, wave functions are increasingly included in these calculations.



With the availability of high energy and high quality beams at CEBAF, the extension of these studies to high transferred momenta and energies can be pursued. Here there is the promise of reaching the transition from hadronic to quark-gluon (or quark and flux-tubes) degrees of freedom. In order to recognize this transition, a consistent “standard nuclear model” for the hadronic degrees of freedom is needed, the breakdown of which will indicate the emergence of the new degrees of freedom. This can be achieved only by providing a large experimental data set with many observables, at various kinematics and on several nuclei to constrain and test the developing models.

### ACKNOWLEDGMENTS

I would like to thank S. Širca and Z.-L. Zhou for their assistance in preparing this manuscript.

### REFERENCES

- [1] L. Lapikas *et al.*, Proc. XV<sup>th</sup> Particles and Nuclei International Conference (PANIC99), Uppsala, 1999, Nucl. Phys. **A663** (2000) 337c
- [2] J.M. Udias *et al.*, <http://xxx.lanl.gov/abs/nucl-th/0101038v.2>
- [3] S. Jeschonnek and R. Schiavilla, Private communications
- [4] S. Jeschonnek and T.W. Donnelly, Phys. Rev. **57** (1998) 2438
- [5] S. Jeschonnek and T.W. Donnelly, Phys. Rev. **59** (1999) 2676
- [6] I. Bobeldijk *et al.*, Phys. Rev. Lett. **73**, No. 20 (1994) 2684
- [7] E.N.M.Quint, Ph.D. thesis, University of Amsterdam (1998) unpublished
- [8] V.R. Pandhripande and S.C. Pieper, Nucl. Phys. **A507** (1990) 167c
- [9] Z.Y.Ma and J. Wambach, Phys. Lett. **B256** (1991) 1
- [10] C. Mahaux and R. Sartor, Adv. Nucl. Phys. **20** (1991) 1
- [11] J.M Udias *et al.*, Phys. Rev. **C53**, No. 4, (1996) R1488
- [12] H. Muther and W.H. Dickhoff, Phys. Rev. **C49**, (1994) R17
- [13] I. Bobeldijk *et al.*, Phys. Lett. **B353**, (1995) 32
- [14] J. Gao *et al.*, Phys. Rev. Lett. **84** (2000) 3265
- [15] J.M. Udias *et al.*, Phys. Rev. Lett. **83** (1999) 5451
- [16] J.J. Kelly, Phys. Rev. **C60** (1999) 044609; the calculations were revised using NLSH wave functions
- [17] T. de Forest Jr., Nucl. Phys. **A392** (1983) 232
- [18] JLab proposal E-00-102, W. Bertozzi, K. Fissum, A. Saha and L. Weinstein, spokespersons
- [19] J.E. Amaro *et al.*, <http://xxx.lanl.gov/abs/nucl-th/0106035>
- [20] J.E. Amaro *et al.*, <http://xxx.lanl.gov/abs/nucl-th/0107069>
- [21] D. Debruyne *et al.*, <http://xxx.lanl.gov/abs/nucl-th/0108012>
- [22] N. Liyanage *et al.*, Phys. Rev. Lett. **86** (2001) 5670
- [23] S. Janssen *et al.*, Nucl. Phys. **A672** (2000) 285
- [24] P.E. Ulmer *et al.*, Phys. Rev. Lett. **59** (1987) 2259
- [25] D. Dutta *et al.*, Phys. Rev. **C61** (2000) 061602(R)
- [26] K.I. Blomqvist *et al.*, Phys. Lett. **B429** (1998) 33
- [27] S.M. Dolfini *et al.*, Phys. Rev. **C60**, No. 6 (1999) 064622
- [28] Z.-L. Zhou *et al.*, <http://xxx.lanl.gov/abs/nucl-ex/0105006>, submitted to Phys. Rev. Lett.
- [29] Update to Bates proposal 89-14, W. Bertozzi, A.J. Sarty, L.B. Weinstein and Z.-L. Zhou spokespersons (1997)
- [30] D. Jordan *et al.*, Phys. Rev. Lett. **76**, No. 10 (1996) 1579
- [31] W. Boeglin, private communication
- [32] R.E.J. Florizone *et al.*, Phys. Rev. Lett. **83** (1999) 2308
- [33] MAMI proposal A1/3-96, R. Neuhausen, spokesperson
- [34] A. Kozlov, contribution to these proceedings
- [35] JLab proposal E-01-020, W. Boeglin, M. Jones, A. Klein, J. Mitchel P. Ulmer and E. Voutier, spokespersons
- [36] JLab proposal E-89-044, M. B. Epstein, R. W. Lourie, J. Mougey, A. Saha, spokespersons
- [37] JLab proposal P-01-108, K. Aniol, S. Gilad, D. Higinbotham and A. Saha, spokespersons